

Baseline Properties and DBTT of High-Burnup PWR Cladding Alloys

Michael C. Billone, Tatiana A. Burtseva, and Yung Y. Liu

Argonne National Laboratory
9700 South Cass Avenue, Argonne, IL 60439, USA

ABSTRACT

Pre-storage drying-transfer operations and early stage storage can subject cladding to high enough temperatures and hoop stresses to induce radial hydride precipitation during long-term dry-cask cooling. These radial hydrides would provide an additional embrittlement mechanism in response to hoop-stress loading during post-storage fuel retrieval and cask transport. Argonne has developed a test protocol for studying high-burnup cladding embrittlement: (1) radial-hydride treatment, during which high-burnup cladding is exposed to simulated drying-storage temperature and stress histories, including slow cooling, and (2) ring compression tests (RCTs), which induce hoop bending stresses in cladding rings that allow determination of strength and ductility as functions of RCT temperature, as well as the ductile-to-brittle transition temperature (DBTT). The protocol was used to generate DBTT data for high-burnup Zircaloy-4 (Zry-4) and ZIRLO™ for the U.S. Nuclear Regulatory Commission and high-burnup M5® for the U.S. Department of Energy (DOE). Under DOE sponsorship, Argonne has also generated baseline properties for the characterization of as-irradiated Zry-4, ZIRLO™, and M5® as well as their RCT strength and ductility. The baseline properties are presented along with a comparison between the strength and ductility of irradiated high-burnup cladding before and after exposure to simulated drying-storage temperature and stress histories.

INTRODUCTION

Cladding mechanical properties and failure limits are needed to assess the behavior of high-burnup (HBU) fuel assemblies during dry-cask storage and transportation. Pre-storage drying-transfer operations and early stage storage can subject cladding to higher temperatures and much higher hoop stresses relative to in-reactor operation and pool storage. During storage, radial hydrides may precipitate in response to slow cooling under tensile hoop stresses. Radial hydrides provide an additional embrittlement mechanism as cladding temperatures decrease below the ductile-to-brittle transition temperature (DBTT).

Argonne has developed a test protocol for studying HBU cladding embrittlement that has been used to generate data for the U.S. Nuclear Regulatory Commission (NRC). Experimentally, the protocol involves two steps: (1) radial-hydride treatment (RHT), during which cladding from HBU fuel rods is exposed to simulated drying-storage temperature and hoop-stress histories, including very slow cooling and decreasing hoop stress, and (2) ring compression tests (RCTs), for which cladding rings are subjected to hoop bending stresses to determine strength and ductility as functions of test temperature. The RCT is used as a ductility screening test and for simulation of pinch-type loading on HBU fuel rods, which occurs during normal conditions of cask transport and/or drop accidents. The protocol was used to generate DBTT data for HBU Zircaloy-4 (Zry-4) and ZIRLO™ (sponsored by the NRC) [1,2] and HBU M5® (sponsored by the U.S. Department of Energy [DOE]) [3]. For these tests, the peak temperature was set at the NRC-recommended limit of 400°C [4], and peak hoop stresses were 110 and 140 MPa at 400°C. For HBU M5®, a sharp transition between brittle (at 60°C) and ductile (at 90°C) behavior was observed for both stress levels. Hydrides that precipitated during cooling were essentially oriented in the radial

direction, with an average length that was 61% (for 140 MPa) and 54% (for 110 MPa) of the cladding wall thickness. The DBTT for M5[®] after RHT was $\approx 75^\circ\text{C}$. For HBU ZIRLO[™], the DBTT was $\approx 185^\circ\text{C}$ and $\approx 125^\circ\text{C}$ for hoop stresses of 140 and 110 MPa, respectively. Concurrent with this decrease in DBTT was a decrease in effective length (as defined by the radial hydride continuity factor [RHCF]) of radial hydrides from 65% (for 140 MPa) to 30% (for 110 MPa) of the cladding wall thickness. For HBU Zry-4 following cooling at 140-MPa peak stress, a smooth transition from brittle to ductile behavior occurred at $\approx 55^\circ\text{C}$. For 110-MPa peak stress, the material was ductile at 24°C and showed a gradual increase in ductility between 24°C and 150°C . Radial hydrides were relatively short (16% RHCF for 140 MPa and 9% RHCF for 110 MPa).

Under DOE sponsorship, Argonne has also generated baseline data on the strength and ductility of as-irradiated HBU M5[®], ZIRLO[™], and Zry-4 cladding from pressurized water reactors (PWRs) [5,6]. Baseline properties were compared to the RCT results for strength (maximum load) and ductility (offset strain) of sibling samples, which were subjected to simulated drying and storage. The results were used to determine the degradation in mechanical properties due to radial hydrides. Baseline properties for as-irradiated HBU cladding are presented in this paper, along with the cladding mechanical performance before and after simulated drying and storage.

CHARACTERIZATION OF AS-IRRADIATED HBU CLADDING

The focus of the characterization effort was to determine the (a) cladding outer diameter (D_o), (b) corrosion layer thickness (h_{ox}), (c) metal wall thickness (h_m), (d) metal outer diameter (D_{mo}), (e) hydrogen content (C_H) of corroded cladding, and (f) C_H within the inner two-thirds of the cladding wall. Cladding segments were about 76-mm long. D_o was measured with a micrometer at several axial locations. Metallographic examination was used to measure h_{ox} and h_m . D_{mo} was determined from $(D_o - 2 h_m)$. Thin cladding rings were heated to melting in a LECO Model RH-404 apparatus to determine C_H . For cladding with a hydride rim, C_H measurements were also performed for samples following removal of the corrosion layer and about one-third of the cladding metal under the corrosion layer. Table 1 summarizes characterization results for as-irradiated HBU M5[®], ZIRLO[™], and Zry-4 segments.

Metallographic examination was used to determine the density and orientation of hydrides across the cladding wall. For M5[®], a recrystallized-annealed (RXA) alloy, some regions were observed with primarily circumferential hydrides and other regions with circumferential and radial hydrides (Fig. 1a). The dissolution temperature for 76-wppm hydrogen is only 306°C [7]. Thus, these hydrides would be dissolved at normal PWR operating conditions, as well as peak drying-storage temperatures. Also, sparsely distributed, short radial hydrides would not contribute to low-temperature embrittlement. In contrast, longer and more closely spaced radial hydrides were observed following cooling at $5^\circ\text{C}/\text{h}$ from the peak drying-storage conditions of 400°C and 140 MPa for HBU M5[®] with 94-wppm C_H (Fig. 1b).

For as-irradiated HBU ZIRLO[™], hydrides were mainly circumferentially oriented and concentrated in the hydride rim (Fig. 2a). The average C_H within the inner two-thirds of the cladding wall was ≈ 140 wppm. This concentration would increase to about 200 wppm at 400°C [7] during drying and storage with essentially no hydrides remaining in this region. Although the cold-work, stress-relief-annealed (CWSRA) microstructure of ZIRLO[™] would make the material less susceptible to radial-hydride precipitation than the RXA microstructure, the relatively low C_H below the hydride rim would increase material susceptibility to radial-hydride precipitation. Long radial hydrides were observed to precipitate in HBU ZIRLO[™] following cooling at $5^\circ\text{C}/\text{h}$ from peak drying-storage conditions of 400°C and 140 MPa for a segment with 650-wppm C_H (Fig. 2b). The longest continuous radial-circumferential hydride, projected onto the cladding radius, in Fig. 2b is $\approx 80\%$ of the wall thickness.

Table 1. Characterization results for HBU cladding segments used in baseline studies.

Parameter	17×17 M5 [®]	17×17 ZIRLO [™]	15×15 Zry-4	
Burnup, GWd/MTU	72	68	67	67
ANL Segment ID	652E6	105A	606C2	605D3
D _o , mm	9.53	9.53	10.75	10.75
h _{ox} , μm	8±1	47±11	95±5	39±5
D _{mo} , mm	9.51	9.44	10.56	10.67
h _m , mm	0.55	0.54	0.69	0.75
C _H (Corroded Cladding), wppm	76±5	530±70	640±140	300±25
C _H (Inner 66% of Wall), wppm	≈76	136±7	246±29	160±7

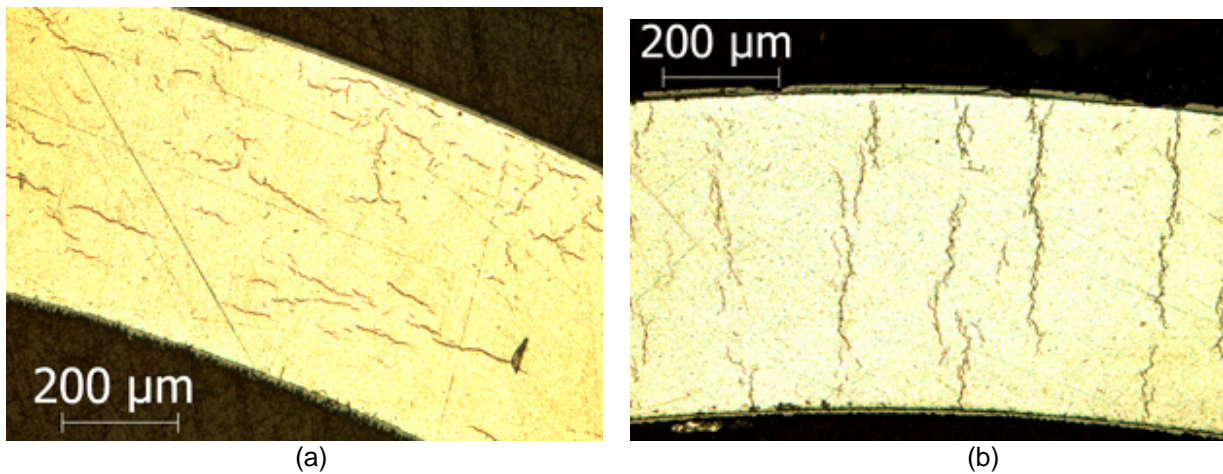


Fig. 1. Hydride morphology in HBU M5[®] cladding: (a) as-irradiated with 76-wppm C_H and (b) following cooling at 5°C/h from 400°C and 140-MPa hoop stress with 94-wppm C_H.

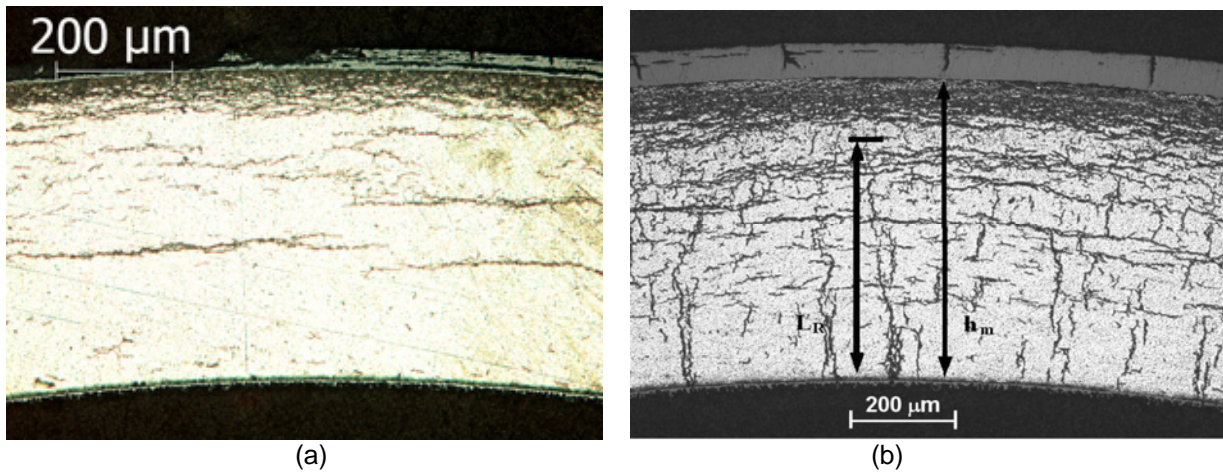


Fig. 2. Hydride morphology in HBU ZIRLO[™] cladding: (a) as-irradiated with 530-wppm C_H and (b) following cooling at 5°C/h from 400°C and 140-MPa hoop stress with 650-wppm C_H.

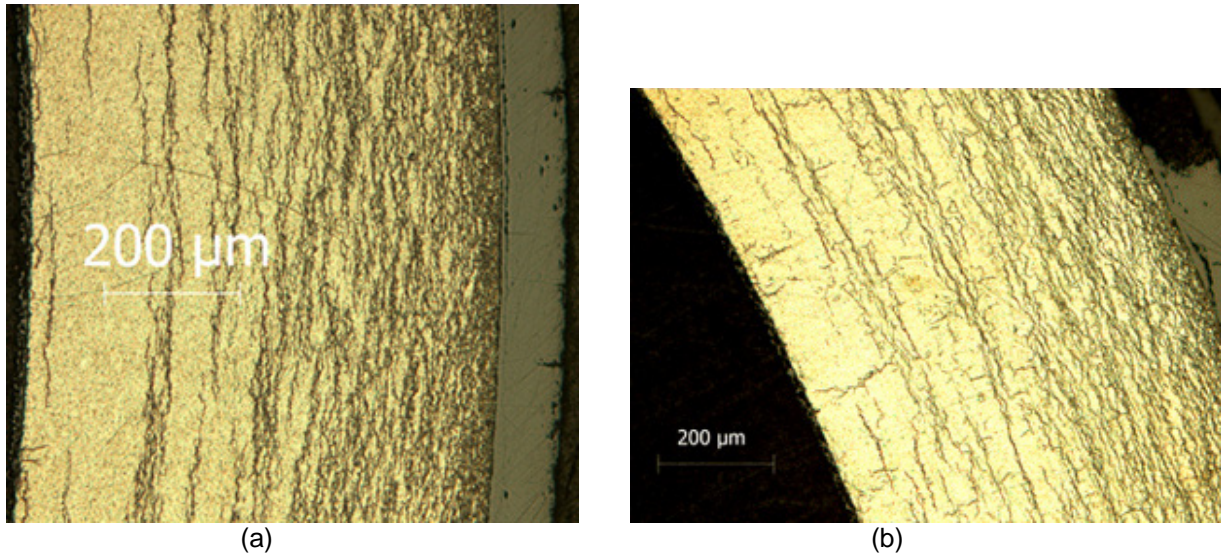


Fig. 3. Hydride morphology in HBU Zry-4: (a) as-irradiated Zry-4 with 640 ± 140 -wppm C_H and (b) following cooling at $5^\circ\text{C}/\text{h}$ from 400°C and 140-MPa hoop stress with 615 ± 82 wppm C_H .

No radial hydrides were found in as-irradiated HBU Zry-4 at ≈ 0.7 m above the fuel mid-span (segment 606C2) and ≈ 0.9 m below the fuel mid-span (segment 605D3). Figure 3a shows the hydride morphology in a high- C_H 606C2 cross section at the 3 o'clock position. Data from quarter-rings at an adjacent position indicated that C_H ranged from 540 wppm to 820 wppm. The high density of hydrides observed in Fig. 3a suggests a local $C_H > 850$ wppm. C_H varied monotonically from the high value at the 3 o'clock position in Fig. 3a to the low value (< 500 wppm) observed at the 9 o'clock position. In contrast to ZIRLO™ (Fig. 2a), hydrides were not as concentrated in the Zry-4 hydride rim. Rather, the more diffuse rim extended as much as 50% into the cladding wall (Fig. 3a). This distribution resulted in 246 ± 29 wppm C_H measured within the inner two-thirds of the cladding wall. The high C_H and the more diffuse hydride distribution would tend to embrittle this cladding at room temperature (RT) due to circumferential hydrides. However, this CWSRA alloy would be less susceptible to radial hydride precipitation because of the presence of circumferential hydrides (about 40 wppm) at 400°C within the inner two-thirds of the cladding wall. The low susceptibility is evident in Fig. 3b for HBU Zry-4 (with 615 ± 82 wppm) following cooling at $5^\circ\text{C}/\text{h}$ from peak conditions of 400°C and 140 MPa.

Segment 605D3 of HBU Zry-4, which was from a lower axial location of a sibling rod, was used to test samples with lower C_H (300 ± 25 wppm). Based on the low C_H , it was anticipated that this material would have high ductility at RT. However, the low C_H (160 ± 7 wppm) within the inner two-thirds of the cladding would tend to make this material more susceptible to radial-hydride precipitation.

RCT RESULTS FOR AS-IRRADIATED HBU CLADDING ALLOYS

RCTs were conducted at RT and displacement rates of 0.05 mm/s, 5 mm/s (reference), and 50 mm/s to study displacement-rate sensitivity. Elevated temperature (60°C to 150°C) RCTs were also conducted at 5 mm/s to study temperature sensitivity. Figure 4 (insert) shows a schematic of RCT loading. This loading induces a maximum bending moment (M_{max}) at the 12 (under load) and 6 (above support) o'clock positions, as well as maximum tensile hoop stresses (σ_θ) and strains (ϵ_θ) at the inner surfaces of these locations. Tensile hoop stresses and strains also occur at the 3 and 9 o'clock outer surfaces. Within the elastic range, the stresses at 3 and 9 o'clock are $\approx 60\%$ of the maximum stresses at 12 and 6 o'clock. Also, because the ring length ($L \approx 8$ mm) is much greater than the wall thickness, an axial stress is induced that

is 0.37 times the hoop stress within the elastic deformation regime. The maximum displacement ($\delta_{\max} = 1.7$ mm) was chosen to give $\approx 10\%$ offset strain at RT.

Load-displacement curves and post-test examination were used to determine offset displacements (δ_p) and permanent displacements (d_p), respectively. These were normalized to D_{mo} to give the relative plastic displacement (i.e., plastic strain) for the ring structure. Permanent displacement is defined as the difference between pre- and post-test diameter measurements along the loading direction. Figure 4 shows how traditional and corrected offset displacements were determined from a benchmark load-displacement curve for a non-irradiated 17×17 M5[®] ring. Results from other benchmark tests indicated that the ratio of unloading stiffness (K_{UM}) to loading stiffness (K_{LM}) decreased with δ_p/D_{mo} . For the 12.6% δ_p/D_{mo} shown in Fig. 4, $K_{UM}/K_{LM} = 0.84$. Based on error analyses and data trends, rings with $d_p/D_{mo} < 1\%$ or $\delta_p/D_{mo} < 2\%$ are classified as brittle.

For rings that crack during 1.7-mm displacement, d_p cannot be determined accurately. Thus, one must rely on the corrected δ_p prior to the first significant crack (>50% of wall) to determine ductility. The embrittlement criterion established for cladding with radial hydrides is $\delta_p/D_{mo} < 2\%$ prior to >25% load drop, which corresponds to a crack occurring through >50% of the wall [1-3].

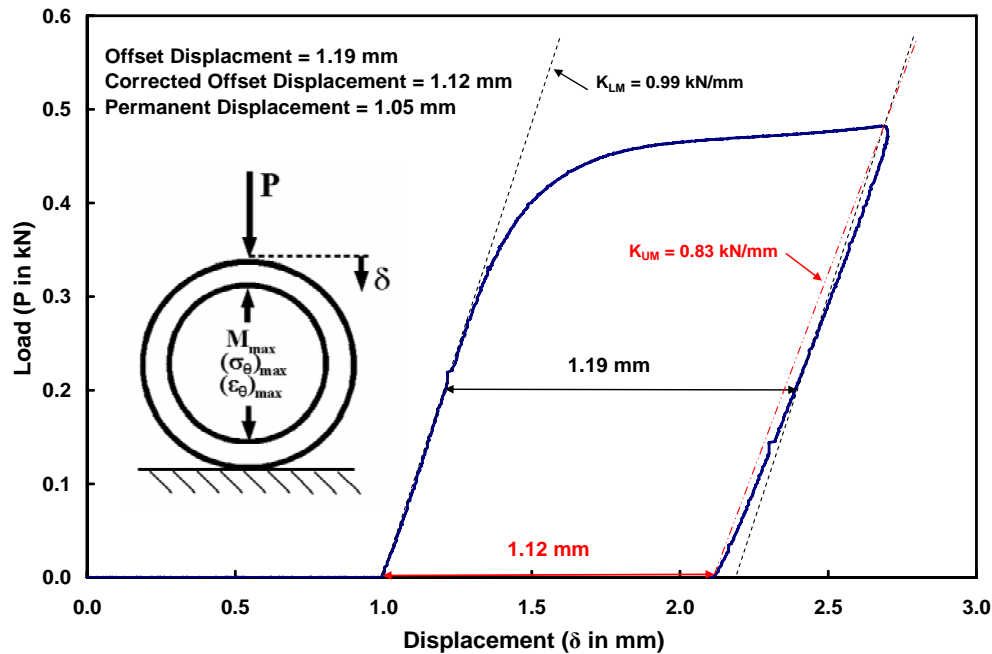


Fig. 4. Load-displacement curve for a non-irradiated 17×15 M5[®] ring tested at RT and 5 mm/s. RCT loading (P) and displacement (δ) are shown in the insert.

RCT Results for As-irradiated HBU M5[®]

Table 2 summarizes RCT results for as-irradiated HBU M5[®]. Rings were 7.6–8.0 mm long. The strength (maximum load P_{\max}) was normalized to 8.0 mm to allow direct comparison of results. As none of the samples cracked, offset and permanent strains represent maximum values attained after 1.7-mm δ . The ductility at RT showed no displacement-rate sensitivity for the 1000-fold increase (from 0.05 to 50 mm/s). The strength increase was relatively small (11%) for the large increase in displacement rate. The strength decrease (9%) with temperature elevation was also modest. Thus, HBU M5[®] exhibited high ductility with relatively low sensitivity to displacement rate and temperature within the conditions tested.

Table 2. RCT results for as-irradiated, high-burnup M5[®] cladding samples.

Sample ID	Length, mm	Displacement Rate, mm/s	RCT Temp., °C	Normalized P _{max} , N	Offset Strain, %	Permanent Strain, %
652E6D	7.86	0.05	26	525	>9.8	>9.1
652E6E	8.02	5	26	553	>9.8	>9.6
652E6K	7.72	50	26	581	>8.7	>8.8
652E6C	7.66	5	60	528	>9.7	>9.5
652E6L	7.62	5	90	506	>10.0	>9.9

RCT Results for As-irradiated HBU ZIRLO™

Table 3 summarizes RCT results for as-irradiated HBU ZIRLO™. Rings were 7.1–8.1 mm long. The RCT at low displacement rate (0.05 mm/s) and RT caused a 39% load drop at ≈7% offset strain. The test was rerun with ring 105A8 and terminated after a 37% load drop at ≈8% offset strain. Two major cracks were observed at the 3 (Fig. 5a) and 9 o'clock orientations, which extended from the outer surface into ≈50% of the wall. Very little change in strength or ductility was observed with the 1000-fold increase in displacement rate: (a) ≈8% increase in strength and (b) ductility decrease from 7.8±0.1.0% to 5.5%. For the ring in the 150°C RCT, there was an increase in ductility and a small (11%) decrease in strength. Cracking occurred near the end of the 90°C RCT: one 60% wall crack and 13 minor cracks (Fig. 5b). Five minor cracks were observed in the 150°C RCT sample. Thus, ductility of as-irradiated HBU ZIRLO™ exhibited some temperature sensitivity.

Table 3. RCT results for as-irradiated HBU ZIRLO™ cladding samples.

Sample ID	Length, mm	Displacement Rate, mm/s	RCT Temp., °C	Normalized P _{max} , N	Offset Strain, %	Permanent Strain, %
105A7	7.90	0.05	20	560	6.7	---
105A8	7.06	0.05	20	529	8.8	---
105A9	7.80	5	20	584	7.0	---
105A10	7.61	50	20	591	5.5	---
105A12	7.52	5	90	553	10.4	---
105A11	8.08	5	150	525	>10.9	>10.2

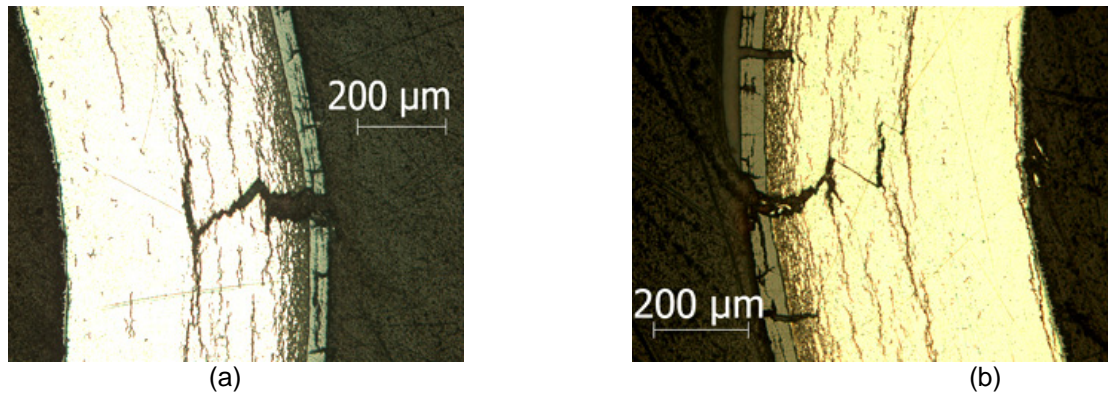


Fig. 5. Crack patterns in post-RCT of HBU ZIRLO™ samples: (a) RT test at 0.05 mm/s terminated after 37% load drop and (b) 90°C test at 5 mm/s to 1.7-mm δ .

RCT Results for As-irradiated HBU Zry-4

Table 4 summarizes RCT results for as-irradiated HBU Zry-4. For high- C_H rings from segment 606C2, the average offset strain was <2% prior to an average load drop of $\approx 30\%$. Sensitivity of ductility to displacement rate and temperature could not be assessed from these data. Based on maximum loads prior to $\approx 30\%$ load drops, strength showed very little sensitivity to displacement rate and temperature (5% decrease at 90°C). The second low-rate RCT was terminated after a 27% load drop. As shown in Fig. 6a, a single crack developed at 9 o'clock, which extended from the outer surface into $\approx 40\%$ of the wall. Two 70% wall cracks developed at 3 (Fig. 6b) and 9 o'clock for the RT test at 5 mm/s to 1.7-mm δ_{max} .

Table 4. RCT results for as-irradiated HBU Zry-4 cladding samples. P_{max} was normalized to 8.0-mm sample length. Sample 605D3F2 had low C_H (300 ± 25 wppm).

Sample ID	Length, mm	Displacement Rate, mm/s	RCT Temp., $^\circ\text{C}$	Normalized P_{max} , N	Offset Strain, %	Permanent Strain, %
606C2G	7.76	0.05	23	989	1.3	---
606C2H	7.81	0.05	20	924	2.3	---
606C2J	7.58	5	23	1010	1.5	---
606C2K	7.97	50	25	996	1.5	---
606C2L	7.69	5	90	958	1.5	---
605D3F2	8.02	5	22	1111	>9.9	>7.6

To verify that the high density of circumferential hydrides caused the embrittlement of the 606C2 samples, an RCT was conducted at RT and 5 mm/s for the lower- C_H (300 wppm) ring 605D3F2. The material exhibited high ductility with no cracking through 1.7-mm δ_{max} . Thus, the HBU Zry-4 metal matrix does indeed have high ductility in response to RCT loading.

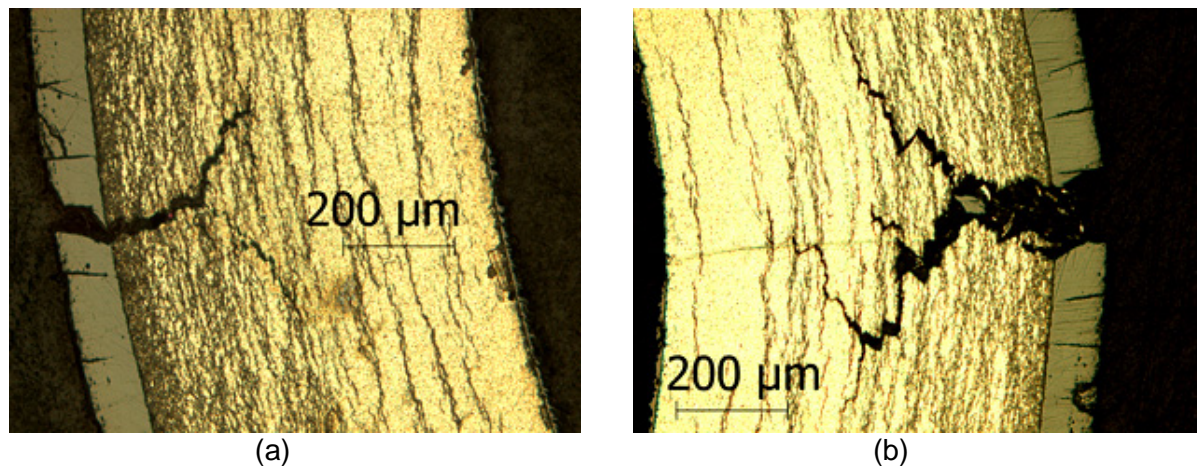


Fig. 6. Crack patterns in as-irradiated HBU Zry-4 after RCTs: (a) single crack for sample tested at RT and 0.05 mm/s and terminated after 27% load drop and (b) one of two major cracks for sample tested at RT and 5 mm/s to 1.7-mm δ .

DEGRADATION OF HBU CLADDING DUE TO DRYING AND DRY-CASK STORAGE

HBU M5[®] Cladding

Ductility values for as-irradiated HBU M5[®] are compared in Fig. 7 to those generated for HBU M5[®] following simulated drying and storage at 400°C and peak hoop stresses of 140 MPa and 110 MPa [3]. Embrittlement for M5[®] following RHT occurred between 60°C and 90°C.

Figure 8 shows the RCT results for as-irradiated M5[®] tested at 26°C and for M5[®] tested at 60°C (below DBTT) after simulated drying and storage at peak conditions of 400°C and 140 MPa. Ductility decreased from >10% to 0% and strength decreased by 52%. For the sample subjected to RHT, failure (>50% wall crack) occurred during elastic loading. Following 1.7-mm δ_{max} , this sample exhibited through-wall cracks at the 3, 6, and 9 o'clock positions and an 80% wall crack at the 12 o'clock position.

Hydrides in high-burnup M5[®], following RHT at 400°C and peak hoop stresses of 140 MPa (Fig. 1b) and 110 MPa, were essentially oriented in the radial direction. The effective length of continuous radial hydrides (RHCF) was $61\pm 18\%$ for 140 MPa and $54\pm 20\%$ for 110 MPa.

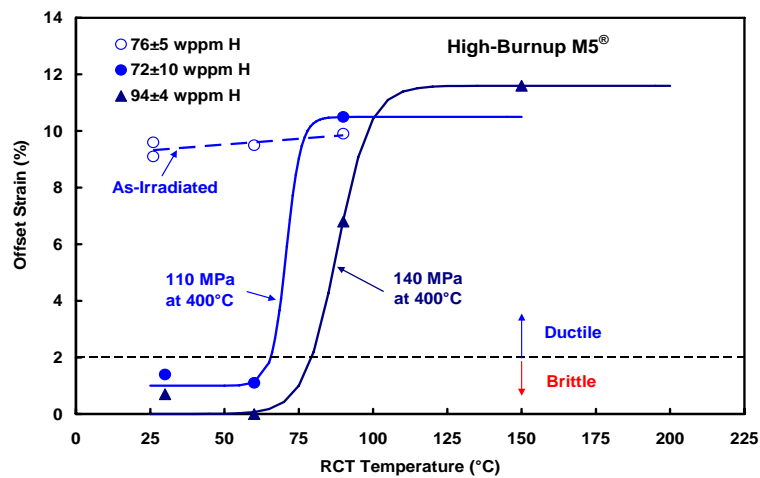


Fig. 7. Ductility comparison for as-irradiated HBU M5[®] and HBU M5[®] following cooling at 5°C/h from 400°C at peak hoop stresses of 110 MPa and 140 MPa.

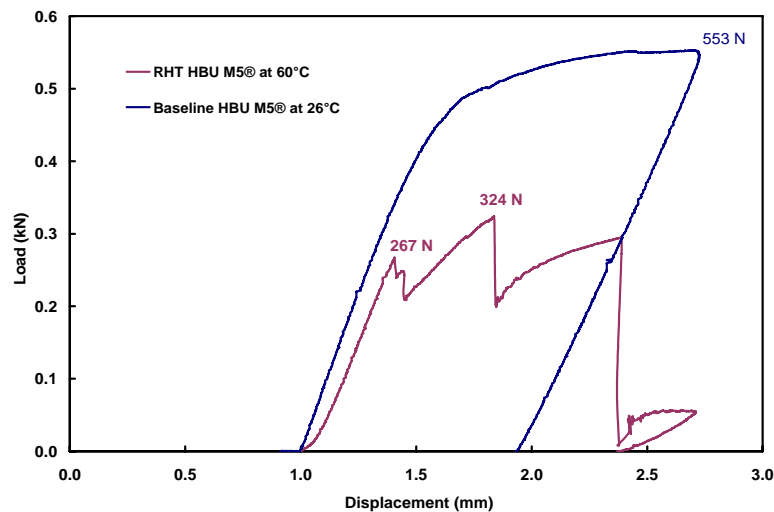


Fig. 8. RCT results for as-irradiated HBU M5[®] tested at 26°C and for HBU M5[®] tested at 60°C following cooling at 5°C/h from 400°C at peak hoop stress of 140 MPa.

HBU ZIRLO™ Cladding

Ductility values for as-irradiated HBU ZIRLO™ are compared in Fig. 9 to those for HBU ZIRLO™ following cooling at 5°C/h from 400°C at peak hoop stresses of 140 MPa and 110 MPa [1]. After RHT, the DBTT for ZIRLO™ was 185°C at 140 MPa and 125°C at 110 MPa.

Figure 10 compares RCT results for the as-irradiated HBU ZIRLO™ sample (530±70 wppm C_H) tested at 20°C and the HBU ZIRLO™ sample (650±190 wppm C_H) tested at 150°C following RHT at 140 MPa. The ring from the RHT segment developed at least one crack extending across >50% of the wall during elastic displacement. The ductility decreased from 7% to 0% and the maximum load decreased by 60%. Long radial hydrides precipitated during slow RHT cooling from 400°C. The effective length of the continuous radial and circumferential hydrides was 65±12% for 140 MPa and 30±12% for 110 MPa.

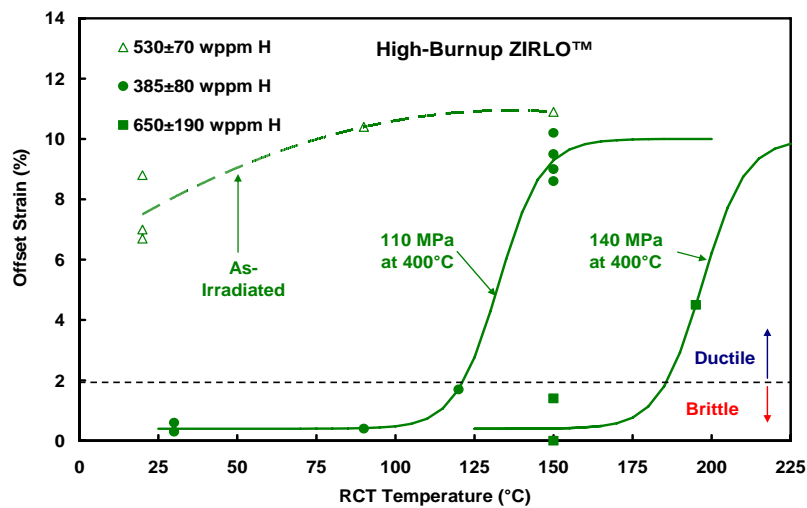


Fig. 9. Ductility comparison for as-irradiated HBU ZIRLO™ and HBU ZIRLO™ following 5°C/h cooling from 400°C at peak hoop stresses of 110 MPa and 140 MPa.

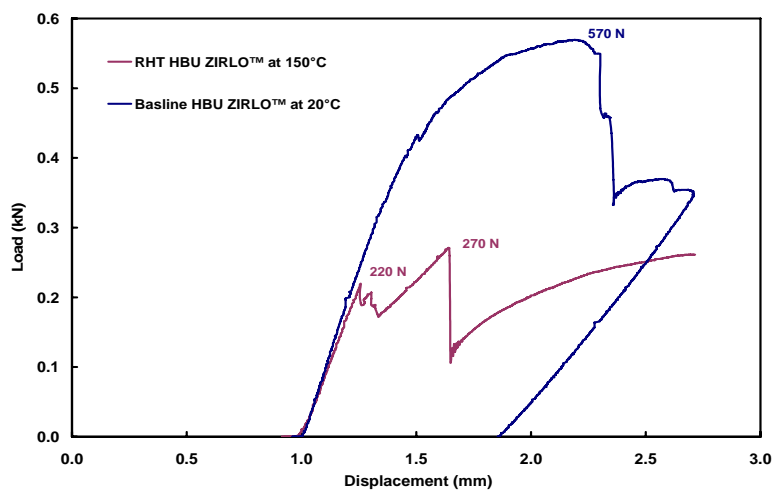


Fig. 10. RCT results for as-irradiated HBU ZIRLO™ tested at 20°C and HBU ZIRLO™ tested at 150°C following 5°C/h cooling from 400°C and 140 MPa.

HBU Zry-4 Cladding

Ductility values for as-irradiated HBU Zry-4 are compared in Fig. 11 to those for HBU Zry-4 following 5°C/h cooling from 400°C and peak hoop stresses of 140 MPa and 110 MPa [1]. The DBTT for Zry-4 was 55°C for 140 MPa and <20°C for 110 MPa. However, the gradual increase in ductility with RCT temperature is not typical of a material that undergoes embrittlement due to radial hydrides. Zry-4 subjected to simulated drying and storage contained short radial hydrides (16% and 9% for 140 MPa and 110 MPa, respectively) that were located closer to the mid-radius than to the inner surface.

Figure 12 compares RCT results for as-irradiated HBU Zry-4 (640±140 wppm C_H) tested at 23°C and HBU Zry-4 (615±82 wppm C_H) tested at 30°C following 140-MPa RHT. Offset strains and strength values were comparable, but the load drop for the RHT sample was larger and more precipitous. Also, the extent of cracking was much greater for the sample following RHT.

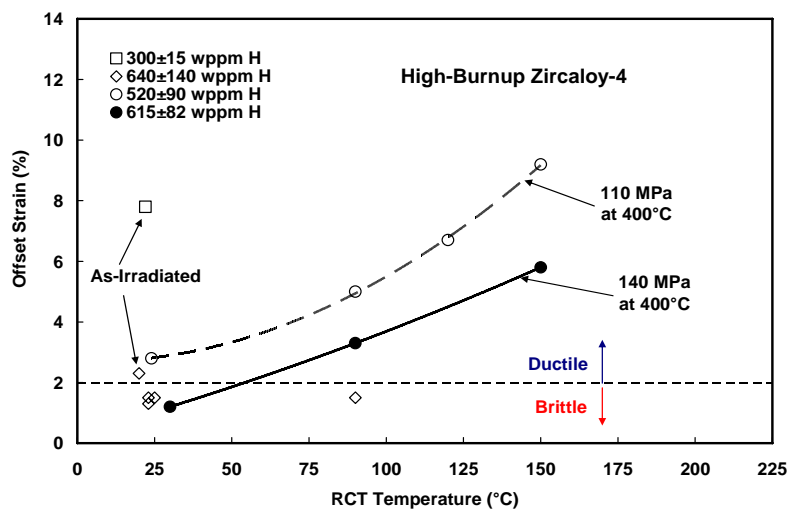


Fig. 11. Ductility comparison for as-irradiated HBU Zry-4 and HBU Zry-4 following cooling at 5°C/h from 400°C at peak hoop stresses of 110 MPa and 140 MPa.

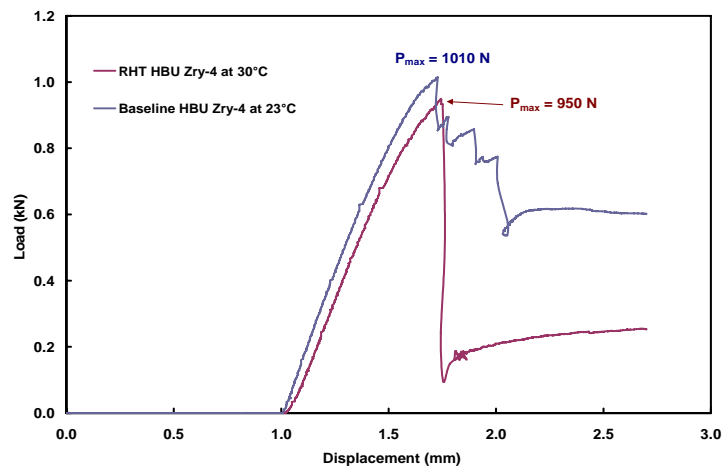


Fig. 12. RCT results for as-irradiated HBU Zry-4 tested at 23°C and HBU Zry-4 tested at 30°C following RHT cooling at 5°C/h from 400°C and peak hoop stress of 140 MPa.

CONCLUSIONS

Baseline RCT results for as-irradiated HBU M5[®] and ZIRLO[™] indicated that these materials have relatively high ductility at RT for displacement rates ranging from 0.05 to 50 mm/s, as well as over a temperature range (26 to 90°C for M5[®] and 20 to 150°C for ZIRLO[™]) relevant to long-term storage. Ductility for these two alloys was relatively insensitive to displacement rate and temperature. As-irradiated HBU Zry-4 with local hydrogen contents >840 wppm exhibited brittle behavior (offset strains < 2%) at RT for the same range of displacement rates, as well as at 90°C and 5 mm/s. Embrittlement was caused by the high density of circumferential hydrides across the outer 50% of the cladding wall. As-irradiated HBU Zry-4 with 300 wppm hydrogen exhibited high ductility at RT and 5 mm/s, which demonstrated the high ductility of the Zry-4 metal matrix. The strengths, as measured by maximum load, of these three PWR alloys exhibited low displacement rate and temperature sensitivity.

However, subjecting these alloys to 5°C/h cooling from 400°C peak drying-storage temperature and peak hoop stress levels of 140 MPa and 110 MPa caused significant reductions in ductility and strength at RCT temperatures below the DBTT. For drying-storage conditions that lead to significant radial hydride precipitation, failure limits used to assess cladding integrity for HBU fuel rods during cask storage and transport should include the degrading effects of radial hydrides.

Additional tests are planned at peak hoop stress of 80–100 MPa and peak temperatures ≤400°C (with and without temperature cycling) to determine DBTT as a function of a wider range of drying-storage conditions. In particular, drying-storage conditions will be determined for which DBTT ≤20°C.

ACKNOWLEDGMENTS

This research was performed at Argonne National Laboratory and supported by the Used Fuel Disposition Campaign, U.S. Department of Energy's Office of Nuclear Energy (NE-53), under Contract DE-AC02-06CH11357. The authors would like to acknowledge Jorge Monroe-Rammsy for his support of this work. The submitted manuscript has been created by UChicago Argonne, LLC, Operator of Argonne National Laboratory ("Argonne"). Argonne, a U.S. Department of Energy Office of Science laboratory, is operated under Contract No. DE-AC02-06CH11357. The U.S. Government retains for itself, and others acting on its behalf, a paid-up nonexclusive, irrevocable worldwide license in said article to reproduce, prepare derivative works, distribute copies to the public, and perform publicly and display publicly, by or on behalf of the Government.

REFERENCES

1. M.C. Billone, T.A. Burtseva, and R.E. Einziger, "Ductile-to-brittle transition temperature for high-burnup cladding alloys exposed to simulated drying-storage conditions," J. Nucl. Mater. 433, 431-448 (2013).
2. M.C. Billone, T.A. Burtseva, and Y. Yan, *Ductile-to-Brittle Transition Temperature for High-Burnup Zircaloy-4 and ZIRLO[™] Cladding Alloys Exposed to Simulated Drying-Storage Conditions*, Argonne Report to NRC, ML12181A238, Sept. 28, 2012.
3. M.C. Billone, T.A. Burtseva, J.P. Dobrzynski, D.P. McGann, K. Byrne, Z. Han, and Y.Y. Liu, *Phase I Ring Compression Testing of High-Burnup Cladding*, FCRD-USED-2012-000039, Dec. 31, 2011.
4. Nuclear Regulatory Commission, "Cladding Considerations for the Transportation and Storage of Spent Fuel," Interim Staff Guidance (ISG)-11, Revision 3 (2003).
5. M.C. Billone, T.A. Burtseva, and Y.Y. Liu, *Baseline Studies for Ring Compression Testing of High-Burnup Fuel Cladding*, FCRD-USED-2013-000040 (ANL 12/58), Nov. 23, 2012.

6. M.C. Billone, T.A. Burtseva, and Y.Y. Liu, "Effects of Drying and Storage on High-Burnup Cladding Ductility," Proc. IHLRWMC, Albuquerque, NM, April 28–May 2, 2013, Paper 6973, 1106-1113 (2013)
7. J.J. Kearns, "Terminal solubility and partitioning of hydrogen in the alpha phase of zirconium, Zircaloy-2, and Zircaloy-4," J. Nucl. Mater. 22, 292-303 (1967).